FLOMEKO 2022

# The comparison of the gas flow primary standard facilities at high pressure

**Chunhui Li[1*], Bodo Mickan[2*], Mengna Li[1], Jia Ren[3], Yan Wu[4], Ming Xu[5]**

*(1, National Institution of Metrology (NIM), Beijing, China,*
*2, Physikalisch-Technische Bundesanstalt (PTB), Braunschweig, Germany,*
*3, Chengdu Natural Gas Sub-Station (Chengdu), Chengdu, China,*
*4, Nanjing Natural Gas Sub-Station (Nanjing), Nanjing, China*
*5, Wuhan Natural Gas Sub-Station (Wuhan), Wuhan, China)*
*Email: lich@nim.ac.cn; bodo.mickan@ptb.de*

**Abstract**

The first formal comparison of gas flow primary standard facilities was conducted in China during 2016~2020. There were 4 participants from China, and PTB was invited as the link lab to connect this comparison with the serial key comparisons of CCM.FF.K5. There were 4 sets of sonic nozzles as the transfer meters, with which there were totally 105 set of measured results were conducted with the Reynolds range ($4.8\times10^4$~$1.1\times10^7$). To cover the Reynolds range, a theoretical equation of discharge coefficient was presented with only one parameter, which was used to evaluate the discharge coefficient at the exact same Reynolds number of the measured points. The evaluation model and uncertainty of the theoretical equation was presented. The degree of equivalence of $E_n$ was finally evaluated. Among all 105 sets of measured results, there were 96 sets of results with $E_n \leq 1$; while there were 8 sets of results with $1 < E_n \leq 1.2$.

## 1. Introduction

Natural gas, oil and coal are the dominant source of primary energy all over the world, which totally take about 80% among all kinds of the primary energy. According to the BP energy outlook: 2020 edition [错误!未找到引用源.], the natural gas is more resilient than for oil, underpinned by the role of natural gas in supporting fast growing developing economies as they decarbonized and reduce their reliance on coal, and as a source of near-zero carbon energy when combined with carbon capture use and storage (CCUS).

For the trade of natural gas, the quantity of flow rate is the most important quantity which is coming from the measurement of flow meter. So, the accuracy of the flow meter in use is the key parameter to guarantee the trade fair, which is generally guaranteed by the regular verification or calibration with the gas flow working standard facility following the quantity value transfer chain as shown in Figure 1.

In China, the coal is the dominant primary energy, which takes over 60% among all kinds of the primary energy and results in serious environment issue. After 2000, the consumption of natural gas has developed rapidly due to the requirement on the low carbon and air pollution. The total consumption was over 300 billion $m^3$ in 2020, whose proportion to the total primary energy was increased to 8% from 4% in 2000. For the natural gas, there is about 2/3 produced in China, and 1/3 imported from other economics. The first natural gas station was built in 1995, which was used to calibrate the flow meter. At present, there are over 10 natural gas stations, among which there are only 3 stations with primary standard facility, i.e., Chengdu station, Nanjing station and Wuhan station.

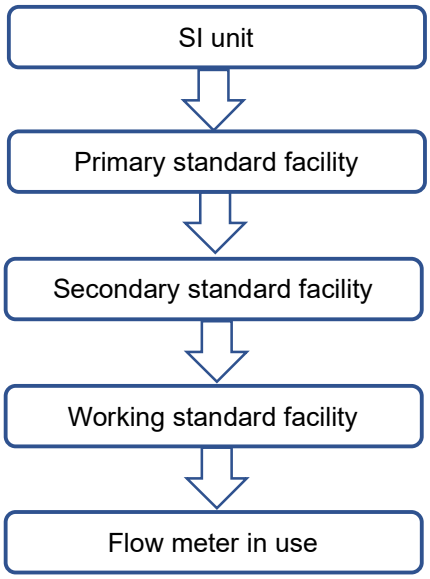


**Figure 1:** the quantity value transfer chain of flow meter

As the national institute of metrology of China (NIM), the gas standard facility of high pressure in NIM was designed in 2010, which was finished at the end of 2014. The maximum pressure is up to 2.5 MPa, and the whole system is consisted with 3 sections,

including: primary standard facility, secondary standard facility and working standard facility.

The natural gas is deeply involved with international trade, commerce, and regulatory affairs, in which it demanded an open, transparency and comprehensive scheme to provide information on the equivalence of national measurement services and the technical basis. CIPM Mutual Recognition Arrangement (CIPM MRA) was the framework through which National Metrology Institutes (NMIs) demonstrate the international equivalence of their measurement standards and the calibration and measurement certificates they issue. The outcomes of the MRA are the internationally recognized Calibration and Measurement Capabilities (CMCs) of the participating institutes. The technical basis of the CIPM MRA is the set of results obtained over the course of time through key comparisons.

The serial comparisons related to the key comparison of CCM.FF.K5, for the working standard facility of gas flow national standard of high pressure were conducted during 2004~2012 [错误!未找到引用源。] to fulfill the requirements of the CIPM MRA, which were all piloted by PTB. The turbines meter with nominal diameter of 150 mm to 300 mm were chosen as the transfer meters, and the degree of equivalence of $E_n$ was evaluated based on the meter deviation.

The comparison for the primary standards facilities was conducted among PTB, LNE, NIM and NIST during 2014~2015[6]. In this comparison, the sonic nozzles were chosen as the transfer meters, and the degree of equivalence of $E_n$ was evaluated based on the discharge coefficient. During 2018~2019, the comparison for the primary standards facilities was conducted among PTB, VSL and Force [7]. In this comparison, the two turbine meters with nominal diameter of 100 mm were chosen as the transfer meters, which were calibrated individually. The degree of equivalence of $E_n$ was evaluated based on the meter deviation.

To achieve the consistence of quantity value for gas flow of high pressure in China, the first formal comparison was organized for the purpose of determination of the degree of equivalence of the primary standards for high-pressure gas flow measurement, which were kept within 2016 to 2020. PTB was invited as the link lab to guarantee the consistence of quantity of value with other economics.

**Table 1:** Participants information

| Country | Labs | Pressure range [kPa] | Working fluid | Date of calibration |
|---|---|---|---|---|
| China | NIM | 100~2500 | Air | September, 2016 to August, 2018 |
| Germany | PTB | 100~5000 | Air<br>Natural gas | November, 2016 to August, 2018 |
| China | Chengdu | 400~5000 | Natural gas | September, 2018 to July, 2020 |
| China | Nanjing | 2000~5000 | Natural gas | March, 2019 |
| China | Wuhan | 5500~7500 | Natural gas | November, 2019 |

As shown in Table 1, the pressure range was quite different for each participant, and the working fluids covered air and natural gas. To analyse the comparison results, the evaluation procedure based on the non-linear least square fit was presented based on Mickan's work [错误!未找到引用源。]. In this paper, the comparison process and evaluation procedure will be presented.

## 2. The comparison schemes

### *2.1 Primary standard facility*

There were 5 participants in this comparison. The technical specification for each primary standard was presented in this section.

#### *2.1.1 NIM*

There are 2 sets pVTt primary standard facilities in NIM. The technical specification of the pVTt facilities is shown in Table 2.

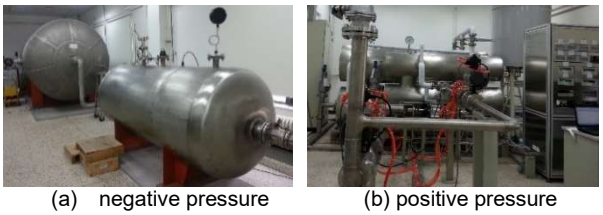

(a) negative pressure (b) positive pressure

**Figure 1:** pVTt facility in NIM

**Table 2:** Technical specification of the pVTt facility in NIM

| Facility | (a) negative pressure | (b) positive pressure |
|---|---|---|
| Volume of collection tank | 2/20 $m^3$ | 0.1/2 $m^3$ |
| Pressure | atmospheric | (100~2500) kPa |
| Temperature | (20±5) ℃ | |
| Flow rate | (1~1300) $m^3/h$ | (0.019~1367) kg/h |
| Uncertainty of MUT | ≥0.10% ($k$=2) | ≥0.08% ($k$=2) |

The tests at atmospheric pressure were conducted in the negative pressure facility, while others were conducted in the positive pressure facility. For the negative pressure pVTt facility, the bilateral comparison between NIM and NIST was conducted between 2008~2009 [9], and the CMC was released in 2013. For the positive pressure facility, the comparison among PTB, LNE, NIST and NIM was conducted in 2015~2016 [6], and the CMC was released in 2019.

#### *2.1.2 PTB*

The tests at atmospheric pressure were conducted in the secondary facility with air, while others were conducted in the HPPP (High Pressure Piston Prover) facility with natural gas. The technical

specification of the HPPP facility is shown in Table 3.

**Figure 2:** HPPP facility in PTB

**Table 3:** Technical specification of the HPPP facility in PTB

| **Pressure** | **(1500~5000) kPa** |
|---|---|
| Temperature | (20±5) ℃ |
| Flow rate | (20~480) $m^3/h$ |
| Uncertainty of MUT | ≥0.065% (*k*=2) |

### *2.1.3 Chengdu*

The tests were conducted in the MT (Mass Time) facility with natural gas [10, 11]. The technical specification of the MT facility is shown in Table 4.

**Figure 3:** MT facility in Chengdu

**Table 4:** Technical specification of the MT facility in Chengdu

| **Volume** | **3.5 $m^3$** |
|---|---|
| Pressure | (300~6000) kPa |
| Temperature | (20±5) ℃ |
| Flow rate | (14.4~19440) kg/h |
| Uncertainty of MUT | ≥0.10% (*k*=2) |

### *2.1.4 Nanjing*

The tests were conducted in the MT facility with natural gas. The technical specification of the MT facility is shown in Table 5.

**Figure 4:** MT facility in Nanjing

**Table 5:** Technical specification of the MT facility in Nanjing

| **Volume** | **10 $m^3$** |
|---|---|
| Pressure | (1500~7500) kPa |
| Temperature | (20±5) ℃ |
| Flow rate | (0.1~8.0) kg/s |
| Uncertainty of MUT | ≥0.15% (*k*=2) |

### *2.1.5 Wuhan*

The tests were conducted in the HPPP facility with natural gas. The technical specification of the HPPP facility is shown in Table 6.

**Figure 5:** HPPP facility in Wuhan

**Table 6:** Technical specification of the HPPP facility in Wuhan

| **Pressure** | **(2500~10000) kPa** |
|---|---|
| Temperature | (20±5) ℃ |
| Flow rate | (20~480) $m^3/h$ |
| Uncertainty of MUT | ≥0.10% (*k*=2) |

### *2.2 Transfer meters and tests*

With consideration of the flow range of the primary standard facilities for all participants, there were four sonic nozzles over the range (8 to 160) $m^3/h$ used as transfer standards, which was shown in Table 7.

**Table 7:** Information of the sonic nozzles

| **SN** | **Nozzle throat diameter [mm]** | **Flowrate [$m^3/h$]** |
|---|---|---|
| 2016-8 | 3.808 | 8 |
| 2016-32-2 | 7.453 | 32 |
| 2016-50 | 9.498 | 50 |
| 2018-160 | 16.361 | 160 |

The discharge coefficient, $C_d$, is used as the comparison parameter [12].

## 3. Comparison results

There were totally 105 sets of measured results. Among them, there were 57 sets of measured points coming from the working fluid of air, while other 48 sets of natural gas. The expanded uncertainty of all the measured results was within (0.074~0.24)% ($k$=2).

### *3.1 Measure results of SN.2016-8*

There were 4 participants made the measured points for this nozzle.

- In NIM: There were 16 sets of pressure, and there were 4 sets of pressure repeated to check the stability of the sonic nozzle.
- In PTB: There were 3 sets of pressure.
- In Chengdu: There were 5 sets of pressure.
- In Nanjing: There were 3 sets of pressure.

### *3.2 Measure results of SN.2016-32-2*

All of 5 participants made the measured points for this nozzle.

- In NIM: There were 19 sets of pressure, and there were 4 sets of pressure repeated to check the stability of the sonic nozzle.
- In PTB: There were 3 sets of pressure.
- In Chengdu: There were 4 sets of pressure.
- In Nanjing: There were 4 sets of pressure.
- In Nanjing: There were 3 sets of pressure.

### *3.3 Measure results of SN. 2016-50*

All of 5 participants made the measured points for this nozzle.

- In NIM: There were 11 sets of pressure.
- In PTB: There were 4 sets of pressure.
- In Chengdu: There were 4 sets of pressure.
- In Nanjing: There were 4 sets of pressure.
- In Nanjing: There were 4 sets of pressure.

### *3.4 Measure results of SN. 2018-160*

There were 4 participants made the measured points for this nozzle.

- In NIM: There were 7 sets of pressure.
- In PTB: There were 4 set of pressure.
- In Chengdu: There were 5 sets of pressure.
- In Wuhan: There were 2 sets of pressure.

## 4. Comparison evaluation and results

### *4.1 Evaluation procedure*

The reference value was determined for each sonic nozzle. Results of all participants were considered for the determination of the reference value and the uncertainty of the reference value.

The challenge for the evaluation of this comparison is caused by the more complex situation regarding the data base and the data processing necessary to satisfy the needs of statistical concepts. The conventional situation for comparisons is:

- Only measurement values generated at the same operation point (regarding flow rate, pressure and gas) are compared, the so-called point-to-point evaluation. The reference value is therefore a single value separated for each operation point.
- Only independent (non-correlated) values are taken into account for the reference value. This requires that each participant provides only one value for each operation point and the comparison is evaluated separately for each operation point.

The situation in this comparison is different because the participants had made their measurements at the operation points according to their possibilities and without a pre-specification of the number of measurements. The consequence is that there is no fixed operation point to be used in the evaluation, but the reference value itself has to be determined as a function of the operation conditions.

### *4.2 Evaluation model*

In 2016, a functionality for the discharge coefficient $C_d$ versus Reynolds number were presented to cover the operating of sonic nozzle with laminar as well as turbulent boundary layers [6, 8].

$$C_{d,fit} = s_{lam} \cdot (a - b_{lam} Re^{-0.5}) + s_{turb} \cdot (a - b_{turb} Re^{-0.139}) \quad (1)$$

where $b_{turb} = 0.003654 b_{lam}^{1.736}$, $s_{turb} = 1 - s_{lam}$

$$s_{lam} = 0.5\left\{1 - \tanh\left[k_u log\left(\frac{Re}{Re_{tr}}\right)\right]\right\} \quad (2)$$

The parameter $Re_{tr}$ represents the middle point of transition and $k_u$ the "sharpness" of the transition (the larger $k_u$, the more "sudden" transition occurs). So, there were three parameters $\{a, b_{lam}, Re_{tr}\}$.

In 2021, with theoretical solutions of Kliegel and Levine [13], Geropp [14,15], the relationship between $a$ and $b_{lam}$ was developed and built [8]. The ratio of Reynolds number at the end of transition and the point where a laminar layer starts to transition (rsp. Is getting instable) can be derived from basic investigations of these issues in high accelerated flows close to transonic condition, for end of transition [18] and point of instability [19]. The outcome is about $\frac{Re_{tr,end}}{Re_{tr,beg}} \approx 2$, so, $k_u = 9.78$ to achieve $\frac{Re_{tr,end}}{Re_{tr,beg}} = 2$, then,

$$Re_{tr} = (1.546 \cdot 10^7 \cdot 0.595^{b_{lam}})/\sqrt{2} \quad (3)$$

The consistency of this relation for the transitional Reynolds number $Re_{tr}$ was verified with several nozzles [20].

Finally, the parameter $b_{lam}$ is the only parameter determining the curve fit of $C_d = f(Re)$.

The vector, $\boldsymbol{C_d}$ of measured values, $C_{d,i}$ for each sonic nozzle is shown as Eq. (4)

$$\boldsymbol{C}_{\mathbf{d}} = (C_{\mathrm{d},i}) = \begin{pmatrix} C_{\mathrm{d},1} \\ \vdots \\ C_{\mathrm{d},n} \end{pmatrix} \quad (4)$$

where $n$ is the quantity of the measured values,
The vector, $\boldsymbol{C}_{\mathbf{d,fit}}$ of fitted values, $C_{\mathrm{d,fit},i}$ for each sonic nozzle at set (vector) Reynolds number $Re_i$ is shown in Eq. (5)

$$\boldsymbol{C}_{\mathbf{d,fit}} = (C_{\mathrm{d,fit},i}) = \begin{pmatrix} C_{\mathrm{d,fit},1} \\ \vdots \\ C_{\mathrm{d,fit},n} \end{pmatrix} \quad (5)$$

The vector, $\boldsymbol{p}$ of all parameters, $p_i$ of the evaluation model is shown as Eq. (6)

$$\boldsymbol{p} = (p_i) = \begin{pmatrix} p_1 \\ \vdots \\ p_{n_p} \end{pmatrix} \quad (6)$$

where $n_p$ is the quantity of the parameters, here only one parameter, $b_{\mathrm{lam}}$.
The Variance-Covariance matrix $\boldsymbol{V_y}$ of the measured values,

$$\boldsymbol{V}_{\boldsymbol{y}} = (v_{i,j}) = \begin{pmatrix} v_{1,1} & \cdots & cov_{i,j} \\ \vdots & \ddots & \vdots \\ cov_{i,j} & \cdots & v_{n,n} \end{pmatrix} \quad (7)$$

where $v_{i,i}$ is the variance, i.e., squared standard uncertainty of the $i^{\mathrm{th}}$ measured point with consideration of installation $C_{\mathrm{d},i}$ and $cov_{i,j}$ the covariance between the $i^{\mathrm{th}}$ and $j^{\mathrm{th}}$ measured point $C_{\mathrm{d},i}$ and $C_{\mathrm{d},j}$.[1]
To evaluate the parameter, $b_{\mathrm{lam}}$, the reduced chi-square value $\chi^2_{\mathrm{red}}$ is used, which is a function of the measured value $C_{\mathrm{d}}$ and the parameters $p$ of the evaluation model used for $C_{\mathrm{d,fit}}$,

$$\chi^2_{\mathrm{red}} = f_{\chi^2_{\mathrm{red}}}(C_{\mathrm{d}}, p) = \frac{1}{\mathrm{DoF}}(\boldsymbol{C}_{\mathbf{d}} - \boldsymbol{C}_{\mathbf{d,fit}})\boldsymbol{W}_{\boldsymbol{y}}(\boldsymbol{C}_{\mathbf{d}} - \boldsymbol{C}_{\mathbf{d,fit}})^{\mathrm{T}} \quad (8)$$

With Gauss-Newton algorithm, the optimal parameter vector, $\boldsymbol{p}_{\mathbf{opt}}$ was determined for the evaluation model, $C_{\mathrm{d,fit}}$, at where the $\chi^2_{\mathrm{red}}$ is the global minimum.

Normalized deviation $E_{\mathrm{n}}$ [16,17] was used to evaluate the consistence of the comparison results, which is defined as,

$$E_{\mathrm{n}} = \frac{|C_{\mathrm{d},i} - C_{\mathrm{d,fit},i}|}{U(C_{\mathrm{d},i} - C_{d,\mathrm{fit},i})} \cong \frac{|bias_i|}{2u_{bias_i}} \quad (9a)$$

where $bias_i = C_{\mathrm{d},i} - C_{\mathrm{d,fit},i}$.

With the optimised parameter $p_{\mathrm{opt}} = b_{\mathrm{lam,opt}}$, the local linear approximation of the design matrix $\boldsymbol{A}$

$$\boldsymbol{A} = \left(\frac{\partial \boldsymbol{c}_{\mathrm{D}}}{\partial b_{\boldsymbol{lam,opt}}}\right) \quad (9b)$$

can be constructed. Together with the Hessian Matrix $\boldsymbol{H}$ from the optimization process with the newton Method, one gets the projection matrix $\boldsymbol{P}$

$$\boldsymbol{P} = \boldsymbol{A} \cdot \boldsymbol{H} \cdot \boldsymbol{A}^{\mathrm{T}} \cdot \boldsymbol{W}_y \quad (9c)$$

and finally, the variance-covariance matrix of the differences $C_{\mathrm{d}} - C_{d,\mathrm{fit}}$

$$\boldsymbol{V}_{C_{\mathrm{d}} - C_{d,\mathrm{fit}}} = (\boldsymbol{I} - \boldsymbol{P}) \cdot \boldsymbol{V}_{C_{\mathrm{d}}} \cdot (\boldsymbol{I} - \boldsymbol{P})^{\mathrm{T}} \quad (9d)$$

The diagonal elements of $\boldsymbol{V}_{C_{\mathrm{d}} - C_{d,\mathrm{fit}}}$ containing our uncertainties of residuals rsp. The differences $C_{\mathrm{d}} - C_{d,\mathrm{fit}}$ for each discharge coefficient $C_{d,\mathrm{i}}$ to the comparison reference curve,

$$u(C_{\mathrm{d,i}} - C_{d,\mathrm{fit,i}}) = \sqrt{v_{C_{\mathrm{d}} - C_{d,\mathrm{fit}},i,i}} \quad (9e)$$

### 4.3 Comparison results

With the above evaluation scheme, the difference between the measured points and the fitted points, $bias$, and the normalized deviation $E_{\mathrm{n}}$. It was clear that the absolute values of the difference were all smaller than 0.20%. Among all 105 sets of measured results, there were 96 sets of results with $E_{\mathrm{n}} \leq 1$, while there were 8 sets of results with $1 < E_{\mathrm{n}} \leq 1.2$.

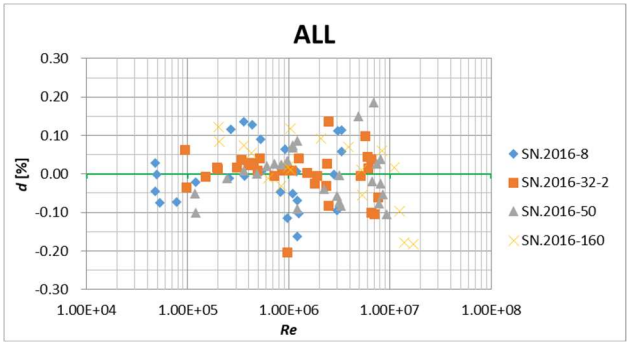


(a) Difference

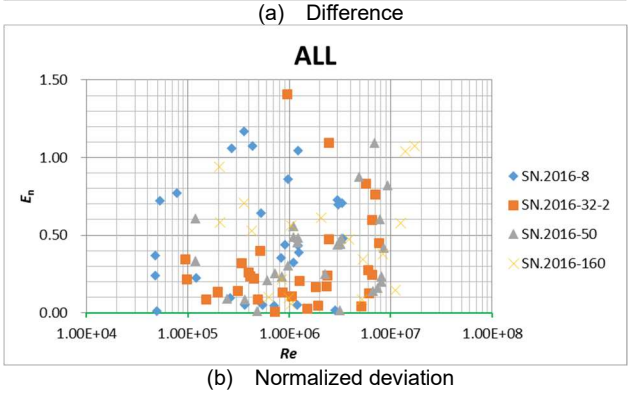


(b) Normalized deviation

**Figure 6:** Comparison results for all participants

#### 4.3.1 NIM results

[1] To evaluate the covariance between the the $i^{\mathrm{th}}$ and $j^{\mathrm{th}}$ measured point $C_{\mathrm{d},i}$ and $C_{\mathrm{d},j}$, the uncertainty from the installation was evaluated as $u_{\mathrm{instal}} = 0.025\%$, and the base uncertainty from the same facility was evaluated as $u_{\mathrm{base}} = 0.02\%$, so, $cov_{i,j} = u^2_{\mathrm{instal}} + u^2_{\mathrm{base}} = 1.025 \times 10^{-7}$.

There were totally 53 sets of results from NIM, the absolute values of the difference were all smaller than 0.15%. Among all 53 sets of measured results,

- There were 50 sets of results with $E_n \leq 1$;
- There were 3 sets of results with $1 < E_n \leq 1.2$ for SN.2016-8.

#### 4.3.2 PTB results

There were totally 14 sets of results from PTB, the absolute values of the difference were all smaller than 0.20%. Among all 11 sets of measured results,

- There were 11 sets of results with $E_n \leq 1$;
- There were 3 sets of results with $1 < E_n \leq 1.2$ for SN.2016-8, SN.2016-32-2 and SN.2016-50 respectively.

#### 4.3.3 Chengdu results

There were totally 18 sets of results from Chengdu, the absolute values of the difference were all smaller than 0.20%. Among all 18 sets of measured results,

- There were 17 sets of results with $E_n \leq 1$;
- There was one set of results with $E_n > 1.2$ for SN.2016-32-2.

#### 4.3.4 Nanjing results

There were totally 11 sets of results from Nanjing, the absolute values of the difference were all smaller than 0.15%. All 11 sets of measured results with $E_n < 1$. The maximum uncertainty, 0.24% ($k$=2) occurred for the measured results of SN.2016-8 at about 2 MPa with Reynolds number $1.25 \times 10^6$, while the uncertainty for all other measured points were no more than 0.148% ($k$=2).

#### 4.3.5 Wuhan results

There were totally 9 sets of results from Wuhan, the absolute values of the difference were all smaller than 0.15%. Among all 9 sets of measured results,

- There were 7 sets of results with $E_n \leq 1$;
- There were 2 sets of results with $1 < E_n \leq 1.2$ for SN.2016-160.

### 4.4 Next step for the comparison

In this comparison, there were totally 105 sets of measured results. 50% of absolute values of the difference were all smaller than 0.04%, and 95% of absolute values of the difference were all smaller than 0.14%. The maximum difference was 0.20%. There was above 95% of $E_n$ value was within the consistent area.

As mentioned before, the participants had made their measurements at the operation points according to their possibilities and without a pre-specification of the number of measurements. Unlike the traditional point-to-point method, there is no fixed operation point to be used in the evaluation and the reference value itself must be determined as a function of the operation conditions. Based on the available literatures, the empirical equation was utilized with only one parameter, $b_{lam}$ to achieve the comparison evaluation as shown in section 4.1. The curve fit was evaluated as shown in Figure 7 as an example.

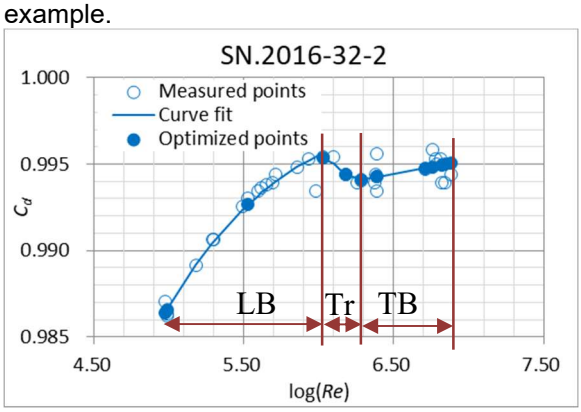


**Figure 7:** Comparison results of SN.2016-32-2

It was clear from Figure 7 that the relationship between Reynolds number and discharge coefficient is different in different boundary layer, such as laminar boundary (LB), transition boundary (Tr) and turbulent boundary (TB). In NIM, the compressed air is used as the working fluid, which is storage in the buffer tank, so the pressure regulated is relatively free. But, the measured results from NIM were mainly located in the laminar boundary region. The correlation among the same participant was considered in the evaluation procedure, however additional uncertainty was occurred. To decrease this effect, the optimized Reynolds number or pressure points will be conducted in the next step. With consideration of the relationship between the Reynolds number and discharge coefficient, and the capability of each participant, the main characteristics of the current curve fit will be the most important factor as shown in Table 8.

**Table 8:** Optimized Reynolds number and pressure for the next step

| | SN | Log(*Re*) | Pressure [kPa] | Working fluid |
|---|---|---|---|---|
| NIM | 1 | 4.97 | 99 | Air |
| | 2 | 5.53 | 348 | |
| | 3 | 6.03 | 1115 | |
| | 4 | 6.18 | 1575 | |
| | 5 | 6.28 | 2028 | |
| PTB | 1 | 4.99 | 100 | |
| | 2 | 6.39 | 2000 | Natural gas |
| | 3 | 6.76 | 5000 | |
| Chengdu | 1 | 5.98 | 822 | |
| | 2 | 6.37 | 2024 | |
| | 3 | 6.71 | 4638 | |
| Nanjing | 1 | 6.39 | 2000 | |
| | 2 | 6.82 | 5537 | |
| Wuhan | 1 | 6.85 | 6341 | |
| | 2 | 6.88 | 7069 | |

## 5. Conclusions

The first formal comparison of gas flow primary standard facilities was conducted in China during 2016~2019. There were 4 participants in this comparison from China, while PTB was invited as the link lab to connect this comparison with the serial key comparisons of CCM.FF.K5. There were 4 sets of sonic nozzles as the transfer meters, with which there were totally 105 set of measured results were conducted with the Reynolds range ($4.8\times10^4$~$1.1\times10^7$). Among them, there were 57 sets of tests coming from the working fluid of air, while other 48 sets of natural gas. There was 99% of expanded uncertainty of the measured results within (0.074~0.148)% ($k$=2), and only one measured results with the maximum of 0.24% ($k$=2). To cover the Reynolds range, a theoretical equation of discharge coefficient was presented with only one parameter, which was used to evaluate the discharge coefficient at the exact same Reynolds number of the measured points. Among all 105 sets of measured results, 50% of absolute values of the difference were all smaller than 0.04%, and 95% of absolute values of the difference were all smaller than 0.14%. The maximum difference was 0.20%. there was above 95% of results within the consistent area.

As the first formal comparison with primary standards facilities of high-pressure gas flow, the current achievement is big milestone. To decrease additional uncertainty from the same participant with consideration of covariance effect, the optimized Reynolds number and pressure points will be fixed in the next step based on the current results.

**Reference**


[1] BP Energy Outlook: 2020 edition.

[2] D. Dopheide, B. Mickan, R. Kramer, et al., Final report on the CIPM Key Comparisons for Natural Gas at High-Pressure Conducted in November / December 2004 CCM.FF-5.a, Metrologia 43, 2006.

[3] D. Dopheide, B. Mickan, R. Kramer, et al., Final report on the CIPM Key Comparisons for Compressed Air and Nitrogen Conducted in November 2004 / June 2005 CCM.FF-5.b, Metrologia 43 07008, 2006.

[4] B. Mickan, D. Dopheide , R. Kramer, et al., Final report on the bilateral CIPM Key Comparison for natural gas at high pressure conducted in October 2006 CCM.FF-K5.a.1, 2007.

[5] B. Mickan, H. Toebben, A. Johnson, et al., Final Results of Bilateral Comparison between NIST and PTB, for Flows of High Pressure Natural Gas, 2006.

[6] Mickan B, Jean-Pierre Vallet, Li C H, J. Wright, “Extended data analysis of bilateral comparisons with air and natural gas up to 5 MPa”, Flomeko, Sydney, 2016.

[7] Arnthor Gunnarsson, Jos van der Grinten, Mijndert van der Beek, Bodo Mickan, Primary Piston Prover Intercomparison Between PTB, VSL and FORCE Technology, Flomeko, Lisbon, 2019.

[8] B. Mickan, Discharge coefficients of CFVN predicted for high Reynolds numbers based on low-Re-calibration, Flow measurement and instrumentation, 101758, 2021.

[9] C.H. Li, Aaron Johnson, The bilateral comparison between NIM’s and NIST’s gas flow capabilities, Journal of Metrology Society of India, 26(3):211-224, 2011.

[10] Jia Rena, Jiqin Duan, Min Huang, Min He, A new mass & time primary standard for natural gas in China and the uncertainty evaluation, Flow measurement and instrumentation, 101567, 2019.

[11] Jia Ren, Jiqin Duan, Yang Dong, Application and uncertainty analysis of a balance weighing system used in natural gas primary standard up to 60 bar, Flow measurement and instrumentation, 101839, 2021.

[12] ISO 9300:2005, Measurement of Gas Flow by Means of Critical Flow Venturi Nozzle.

[13] J.R. Kliegel, J.N. Levine, Transonic flow in small throat radius of curvature nozzles, AIAA J. 7 (7) (1969) 1375–1378.

[14] D. Geropp, Laminare Grenzschichten in ebenen und rotationssymmetrischen Lavalduessen, Deutsche Luft- und Raumfahrt, Forschung, 71–90, 1971.

[15] Geropp, Laminare Grenzschichten in Überschalldüsen, Deutsche Luft- und Raumfahrt, Forschungsbericht 01 TM 8603-AK/PA 1, 1987.

[16] Cox M.G., Evaluation of key comparison data. Metrologia, 39, 589-595, 2002.

[17] Cox M.G., The evaluation of key comparison data: determining the largest consistent subset, Metrologia, 44, 187-200, 2007.

[18] A. Demetriades, Roughness Effects on Boundary-Layer Transition in a Nozzle Throat, AIAA 81-4087

[19] W. Albring, Angewandt Strömungslehre, Verlag Theodor Steinkopff, Dresden, Germany, 1970

[20] B. Mickan, Determination of Discharge Coefficient; based on Shape Measurement in Sonic Nozzles - Experience at PTB, Workshop on the state-of-the-art regarding CFVNs, EMPIR project MetHyInfra, 2022-09-16, Online

**Annex 1: Comparison with and without consideration of covariance to estimate impact of covariance on $E_n$**

The covariance effect was considered in the analyses of the comparison as shown in section 4.2.1. The impact of covariance on $E_n$, $\Delta E_n$ was evaluated as Eq. (1-1)

$$\Delta E_n = E_{n,no} - E_{n,cov} \quad (1\text{-}1)$$

Where $E_{n,cov}$ is the $E_n$ value with consideration the effect of covariance, $E_{n,no}$ is the $E_n$ value without consideration the effect of covariance. The comparison was shown in Figure 1-1

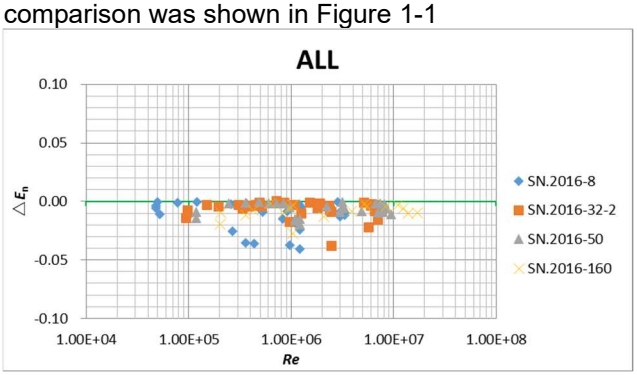


**Figure 1-1:** Comparison between with and without covariance effect

As mentioned in section 4.1.3, the covariance between the the $i^{th}$ and $j^{th}$ measured point $C_{d,i}$ and $C_{d,j}$, was evaluated with the uncertainty from the installation as $u_{instal} = 0.025\%$, and the base uncertainty from the same facility as $u_{base} = 0.02\%$, so, $cov_{i,j} = u_{instal}^2 + u_{base}^2 = 1.025 \times 10^{-7}$. The diagonal element in Eq. (7) was coming from the uncertainty of each measured point with consideration of installation, $v_{i,i}$ = [(0.037%)²+(0.025%)²]~ [(0.12%)²+(0.025%)²] = $1.994\times 10^{-7}$~$1.503\times 10^{-5}$. Hence, the correlation coefficients $r_{i,j} = v_{i,j}/\sqrt{v_{ii}v_{jj}}$ vary between 0.02 and 0.52. So, the effect of covariance was not strong. However, the ignorance of covariances will lead to an underestimation of $E_n$ values, the maximum covariance effect on the $E_n$ could be 0.04 in this comparison. The consideration of the covariances effect is necessary.

**Annex 2: Impact of installation resulted from the size of temperature sensing element based on experience of Nanjing**

There are detailed requirements in the regulation of ISO 9300 [12] on the temperature measurement. When an upstream pipeline is used the recommended location of these sensors is 1.8*D* to 2.2*D* upstream of the inlet plane of the CFVN. The diameter of the sensing element shall be not larger than 0.04*D* and the element shall not be aligned with a wall pressure tapping in the flow direction. If it is impracticable to use a sensing element of diameter less than 0.04*D*, the sensing element shall be so located that it can be demonstrated that it does not affect the pressure measurement.

- **Installation condition 1**

The diameter of sensing element is 4 mm, while the diameter of the pipeline is 100 mm, which is satisfied with requirement of not larger than 0.04*D*. So, in the comparison analyses, the results from the installation condition 1 were utilized.

- **Installation condition 2**

The sensing element is installed in the thermal well with the diameter of 10 mm, which is not satisfied with the requirement of not larger than 0.04*D*.

At the similar Reynolds number, the difference of discharge coefficient between the different installation condition, $\Delta C_d$, was evaluated as,

$$\Delta C_d = C_{\mathrm{d},T2} - C_{\mathrm{d},T1} \quad (2\text{-}1)$$

Where $C_{\mathrm{d},T1}$ referred the discharge coefficient from the installation condition 1, $C_{\mathrm{d},T2}$ referred the discharge coefficient from the installation condition 2. The results were shown in Figure 2-1,

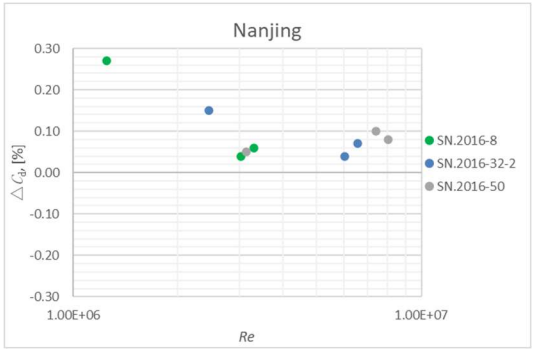


**Figure 2-1:** Installation effect of temperature sensing element

It was clear that all the differences were positive, and temperature effect was significant at relative low Reynolds number, which could be 0.27%, while it remained within 0.1% at relative higher Reynolds number.

When the tests were conducted in PTB with natural gas, the diameter of the pipeline was 50 mm, while the diameter of the temperature sensing element was 8 mm which was installed about 3.5*D* upstream of the inlet plane of the CFVN. The obviously increase of discharge coefficient occurred for the biggest nozzle, i.e., SN. 2018-160.

Combination the experience from Nanjing and PTB, the additional corrections for the stagnation parameters are required when the requirement of the diameter of the sensing element is larger than 0.04*D*, whose effect shows stronger with the bigger ratio between the diameter of temperature sensing element to the diameter of pipeline, and the effect will be qualified in the future.